Isothermal Crystallization of End-Linked Poly(tetrahydrofuran) Networks. 2. Molecular Weight Dependence

Hiroshi Takahashi, Mitsuhiro Shibayama,* Manabu Hashimoto, and Shunji Nomura

Department of Polymer Science and Engineering, Kyoto Institute of Technology, Matsugasaki, Sakyo-ku, Kyoto 606, Japan

Received December 29, 1994; Revised Manuscript Received April 12, 1995[⊗]

ABSTRACT: The slow crystallization kinetics of model networks consisting of end-linked poly(tetrahydrofuran) (PTHF) was investigated as a function of the prepolymer molecular weight, M_n. The crystallization half times, $t_{1/2}$, estimated by both differential scanning calorimetry (DSC) and small-angle X-ray scattering (SAXS), were in good agreement with each other. It was found that $t_{1/2}$ was very sensitive to M_n, ranging from 40 to 400 min when crystallized at 15 °C. This strongly indicates depression of the capability of crystallization by the introduction of cross-links. The role of cross-links on isothermal crystallization is discussed from both kinetic and thermodynamic points of view.

Introduction

Crystallization of polymer networks is very different from that of linear polymers because diffusion of molten polymer chains participating in crystallization is greatly restricted due to the presence of cross-links. Furthermore, exclusion of cross-links from the crystalline phase leads to depression of the degree of crystallization as well as the rate of crystallization. Phillips and coworkers studied the crystallization kinetics of statistically cross-linked polyethylene by a depolarized light scattering method[1,2] and by small-angle X-ray scattering (SAXS).[3] It was found that the crystallization rate was greatly suppressed by increasing the cross-link density. In the case of polymer networks, two major terms affecting crystallization have to be taken into account: (i) depression of polymer chain diffusion and (ii) changes in the interfacial free energy at the crystal–melt interface due to the presence of cross-links.

Recently, we reported the slow crystallization kinetics of an end-linked poly(tetrahydrofuran) (PTHF) network having a narrow inter-cross-link molecular weight distribution (part 1 of this series).[4] A PTHF prepolymer, prepared by cationic living polymerization of tetrahydrofuran (THF), had $M_n = 5.2 \times 10^3$ and a polydispersity index, M_w/M_n, of 1.17, where M_w and M_n, respectively, denote the weight and number average molecular weights. Then the PTHF network was obtained by chain coupling with a four-functional cross-linker. Two surprising results were obtained for this PTHF network: (1) It took about *1 week* to complete crystallization at 20 °C. (2) *Spherulites* were observed by light scattering and optical microscopy although the number of monomers between cross-links was about 70. This slow crystallization enabled us to study the crystallization kinetics with differential scanning calorimetry (DSC) since the DSC heating rate was much faster than the crystallization rate. The results were in good agreement with those obtained by an independent method, i.e., infrared absorption spectroscopy. However, morphological studies on this system have not been conducted although the formation of spherulite texture stimulates our curiosity about the crystallization mechanism of polymer networks. In addition, the sol fraction was not removed from the system, which was expected to play a significant role in crystallization.

Time-resolved small angle X-ray scattering (SAXS) and wide angle X-ray diffraction (WAXD) became common tools for quantitative investigations of polymer crystallization. These are owing to rapid advances in technology, such as the brilliant X-ray source from synchrotron orbital radiation, highly efficient X-ray detection with linear position detectors or area detectors (imaging plate), and related computer technology. Therefore, it is now feasible to study rapid crystallization kinetics of polymers[3,5–7] including more sophisticated systems, such as polymer blends[8,9] and block copolymers.[10] In order to obtain quantitative information about the crystallization of network polymers, SAXS (and/or WAXD) should be employed to study the crystallization of network polymers. The slow crystallization described above, however, does not benefit from such technology because of a limitation of beam time. Thus, as will be discussed below, we planned to raise the crystallization rate of the PTHF network of $M_n = 5.2 \times 10^3$ by lowering the crystallization temperature from 20 to 15 °C. This temperature was chosen on the basis of a preliminary experiment of crystallization at various temperatures by the depolarized light scattering method.[1,2] Furthermore, the sol portion was removed from the as-prepared network polymers since nucleation could be inititated from the sol part of the as-prepared network. Actually, the crystallization rate of the sol-free network was suppressed by a factor of ~2 at the same crystallization temperature. Thus a time range for this crystallization of less than 1 day was attained.

In this paper, we present results of crystallization kinetics obtained by DSC for the postcrystallized PTHF network and by real-time SAXS as well as optical microscopy for the PTHF network during crystallization. Then the effect of cross-links on crystallization is discussed.

Experimental Section

1. Samples. PTHF networks were prepared by a two-step reaction; prepolymer polymerization and chain coupling. A series of prepolymers were synthesized by living cationic polymerization of tetrahydrofuran terminated by allyl alcohol at both ends. Then the prepolymers were end-coupled with a four-functional cross-linker, pentaerythritol tetrakis(3-mercaptopropionate), purified grade, Aldrich Chemical Co. The details of sample preparation are described elsewhere.[4,11] Table 1 shows the characterization of thus-prepared PTHF unimodal networks. Columns 2–5 are the characteristics of

* To whom correspondence should be addressed.

[⊗] Abstract published in *Advance ACS Abstracts,* July 1, 1995.

0024-9297/95/2228-5547$09.00/0

Table 1. Characterization for Prepolymers and Gel Fraction for As-Prepared Networks

sample code	prepolymer				gel fraction
	$10^{-3}M_n$[a]	x_n	M_w/M_n[b]	functionality[c]	
U025	2.54	34.1	1.15	1.85	0.95
U044	4.36	59.3	1.17	2.02	0.90
U052	5.19	70.8	1.17	1.94	0.91
U065	6.48	88.7	1.22	1.83	0.90
U079	7.91	109	1.18	1.94	0.81
U102	10.2	140	1.20	2.09	0.70
E102	10.2	140	1.20	2.09	

[a] By VPO. [b] By GPC. [c] By ^{1}H-NMR.

the corresponding prepolymers used for the preparation of networks, and column 6 is the gel fraction of the PTHF networks after the cross-link reaction. The numbers on the sample codes indicate the number average molecular weight, M_n, of the prepolymers evaluated by vapor pressure osmometry (VPO, Knauer). The range of M_n's is from 2.54×10^3 to 10.2×10^3. x_n is the degree of polymerization of PTHF between successive cross-links evaluated from M_n. The polydispersity index, M_w/M_n, was obtained with gel permeation chromatography (GPC). Owing to an employment of living cationic polymerization, M_w/M_n was reasonably small compared with one obtained by radical polymerization. The functionality of the allyl end group was determined by ^{1}H-NMR (a 300 MHz QE-300 NMR spectrometer, General Electric), which was close to the value of the stoichiometric value of 2. The gel fraction of the PTHF network after the cross-link reaction was obtained by weighing the soluble portion of the PTHF network in toluene. The gel fraction decreased systematically with increasing M_n. P102 and E102 are the prepolymer of U102 and a chain-extended polymer by using a two-functional reagent, ethylene glycol bis(thioglycolate), respectively. These two polymers were used as reference samples. Sol-fraction-free network polymers were used for the experiments.

2. DSC. Samples of about 3 mg were crimped in an aluminum pan and heat treated at 60 °C, which was higher than the melting temperature of PTHF, and then the samples were aged at a crystallization temperature of T_C = 15 °C for a given crystallization time, t. Differential scanning calorimetry (DSC) was carried out with a DSC 3100 (MAC Science Co. Ltd., a heat flux type DSC). The heating rate was 5 °C/min. For T_C dependence experiments, heat-treated samples were quickly loaded in a temperature-controlled chamber of which the temperature was kept constant at the crystallization temperature, T_C. After completion of crystallization at T_C, DSC thermograms were obtained.

3. SAXS and Optical Microscopy. Real-time crystallization kinetics of the PTHF networks and prepolymers were also studied by small-angle X-ray scattering (SAXS). The SAXS experiments were conducted with a high brilliant X-ray beam from synchrotron orbital radiation, National Laboratory for High Energy Physics, Tsukuba, Japan. Sample films of 500 μm thickness were heat treated at 60 °C and then quickly transferred to a temperature-controlled chamber kept at 15 °C, followed by a time-resolved SAXS experiment. The wavelength of the X-ray was 1.488 Å. The sampling time was either 5 min or 1 min each, depending on the rate of crystallization. The details of the experimental setup as well as of the data correction are described elsewhere.[12] Spherulite growth of the network polymer films of about 100 μm thick was observed with an optical microscope under cross polarization, which was coupled with a set of a CCD (charge-coupled device) camera and scaler for an accurate determination of the spherulite size. In both cases, the samples were mounted in a water-circulated temperature-controllable chamber and the temperature was regulated with a RTE-110D (Neslab Instruments, Inc.). The precision of the temperature regulation was about ±0.1 °C.

Results

1. Crystallization Kinetics. Figure 1 shows the DSC thermograms of U052 crystallized for different crystallization times, t. The dashed curve in the figure is a thermogram for P052 (the prepolymer of U052) crystallized at the same temperature for 1440 min (24 h). The crystallization temperature was 15 °C. It should be noted that the glass transition temperature of PTHF is about −86 °C.[13] Thus it is not necessary to take into account the glass transition of PTHF for the discussion of the crystallization at 15 °C. The endothermic peak located at about 30 °C corresponds to the melting endotherm of PTHF, which becomes larger with increasing t. From this figure, it is obvious that both the melting temperature, T_m, and the enthalpy of fusion, ΔH, of PTHF, are remarkably depressed and broadened by the introduction of cross-links.

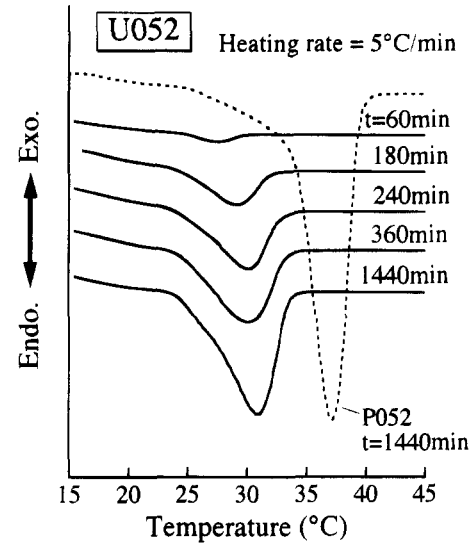

Figure 1. Crystallization time dependence of DSC thermograms of U052 (PTHF network). The dashed curve indicates a DSC thermogram for P052 (prepolymer) crystallized for t = 1440 min. The crystallization temperature, T_c, was 15 °C.

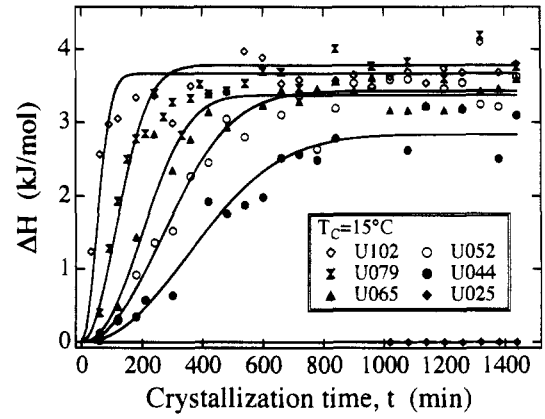

Figure 2. Crystallization time dependence of the enthalpy of fusion of PTHF networks, ΔH. Curves are shown for the eye.

Figure 2 shows the variations of the melting endotherm, ΔH, as a function of t for PTHF networks crystallized at T_C = 15 °C. In the case of U025, no endotherm was observed. However, all of the other networks having higher M_n were found to be crystallizable at this temperature. The rate of crystallization was faster for the PTHF network having a higher M_n. We should make two notes here: (1) the isothermal crystallization rate of a PTHF network is suppressed by extracting the sol fraction from the network, and (2) even U025, having only 34 monomer units between cross-links, is crystallizable when T_C is lowered to 0 °C.[14]

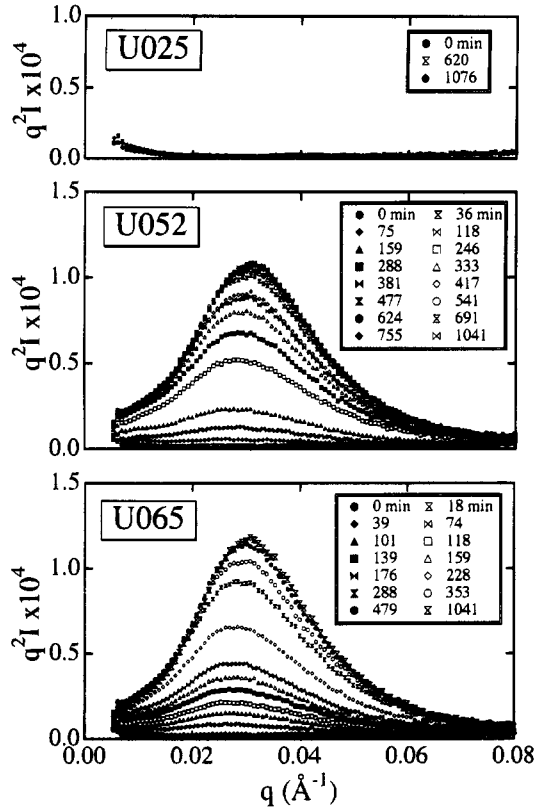

Figure 3. Lorentz-corrected SAXS intensity profiles of U025, U052, and U065 during crystallization.

Figure 3 shows the Lorentz-factor-corrected scattered intensity function $q^2I(q)$ vs q plots of the networks, U025, U052, and U065. The Lorentz factor correction is made because the samples can be assumed to consist of randomly oriented crystallites.[15] The quantity q is the magnitude of the scattering vector defined by $q = (4\pi/\lambda) \sin \theta$, where λ and 2θ are the wavelength of the X-ray and the scattering angle, respectively. Although no peak evolution with time was detected for U025, an evident peak growth due to crystal formation and its ordering was observed for U052 and U065. Behaviors similar to those of U052 and U065 were also observed in U079 and U102. These scattering peaks indicate the presence of an ordered structure, presumably stacked lamellae having a long period of about 200 Å.

The long period, L, and lamellar thickness, d, can be evaluated by taking the Fourier transform of the Lorentz-corrected scattered intensity function, which generates a one-dimensional correlation function, $\gamma(r)$, defined by[16]

$$\gamma(r) = \frac{\int q^2 I(q) \cos(qr)\, dq}{\gamma(0)} \qquad (1)$$

Extrapolations of $I(q)$ to zero and infinite q were conducted by using a Gaussian function ($q \to 0$) and $I(q) \sim q^{-4}$ ($q \to \infty$; Porod law), respectively. Figure 4 shows $\gamma(r)$ for U052. For $t \geq 118$ min, oscillation of $\gamma(r)$ becomes stable, indicating a structural transition from ill-organized crystallites to stacked and/or aligned crystallites. The long period L and lamellar thickness d were then estimated on the basis of the method of Strobl,[16] i.e., from the value of r at the maximum of $\gamma(r)$ and from the value of the intersection of the tangent of $\gamma(r)$ with the base line, $B = -X_c/(1 - X_c)$, respectively. X_c is the degree of crystallinity and is estimated from

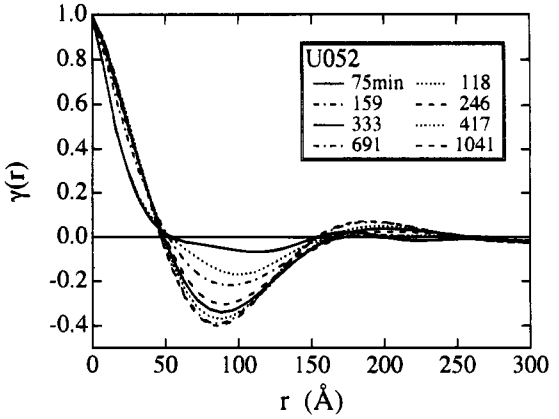

Figure 4. One-dimensional correlation function, $\gamma(r)$, for U052 crystallized for several crystallization times, t.

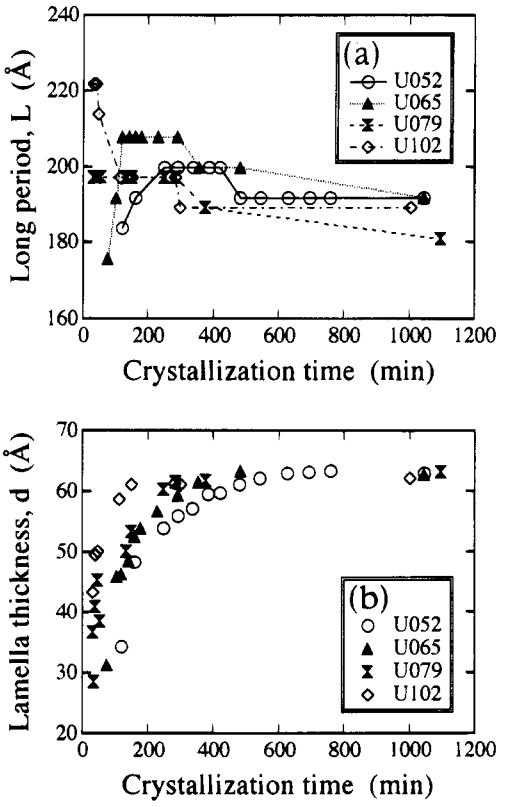

Figure 5. Crystallization time dependence of (a) the long period, L, and (b) the lamellar thickness, d.

the DSC data in this work. The variation of L and d are shown in Figure 5a,b, respectively. L decreases slightly with crystallization of time t for $t > 200$ min. Similar analyses were conducted by several groups,[3,5,6] among which Chu et al.[6] reported a result similar to ours, i.e., a slight decrease in L with t. Though the analysis gives an increase in d for $0 < t < 400$ min, this seems to be an artifact resulting from the interpretation of the correlation function. Since the crystallization took place isothermally, lamellar thickening was not expected during crystallization. The important finding is that the lamellar thickness becomes independent of x_n for larger t. The long period L seems to be about 200 Å and is also independent of x_n, as shown in Figure 6. These values are consistent with the values determined by the peak positions in the $q^2I(q)$ vs q plot. Note that the L's of P102 and E102 are about 140 and 155 Å, respectively. Formation of crystal lamellae having a smaller long period may result from the fact that

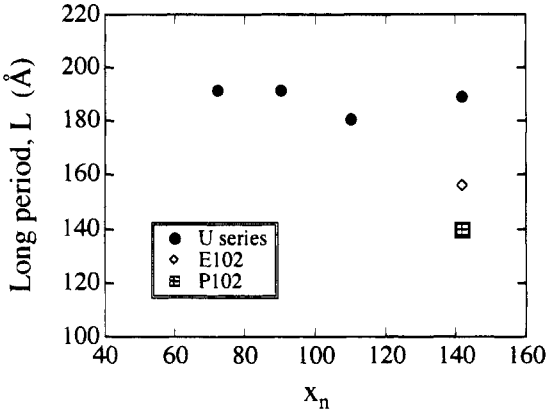

Figure 6. Variation of L with the degree of polymerization between cross-links, x_n.

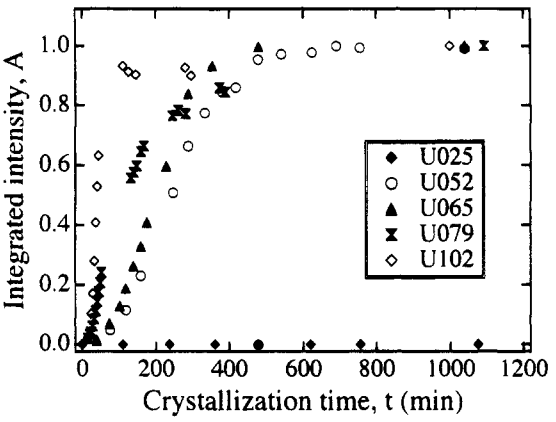

Figure 7. SAXS integrated intensity, A, variation as a function of crystallization time.

crystallization of P102 and E102 is faster than networks.

For an evaluation of the degree of crystallization and/or the degree of crystal ordering, the integrated intensity, A, is defined by

$$A = \int_{q_{min}}^{q_{max}} Iq^2\, dq \qquad (2)$$

where q_{min} and q_{max} were chosen to be 0.006 and 0.08 Å^{-1}, respectively. A is related to the invariant, Q,

$$A \approx Q = \phi_c(1 - \phi_c)(\Delta\varrho)^2 \sim \gamma(0) \qquad (3)$$

since the major contribution to Q is from the scattering maximum in the SAXS profiles. In eq 3, ϕ_c and $\Delta\varrho$ are the volume fraction of the crystalline phase and the electron density difference between the crystalline and amorphous phases.

Figure 7 shows the variation of the integrated scattered intensity, A, with t. By comparing network polymers (U052 to U102), a systematic variation in the kinetics of crystallization with M_n is found. The higher M_n, the faster the crystallization rate is. The similarity in M_n dependencies of ΔH and of A is clearly seen in Figure 8, where the crystallization half time $t_{1/2}$ for the networks (U series) as well as the corresponding polymers, E102 and P102, is plotted as a function of M_n. The agreement in $t_{1/2}$ obtained by DSC and SAXS suggests that the crystallization kinetics of PTHF networks was properly evaluated by these methods in spite of the difference in the experimental setups, i.e., postcrystallization (DSC) and real-time crystallization experiments (SAXS). It is also noteworthy here that $t_{1/2}$

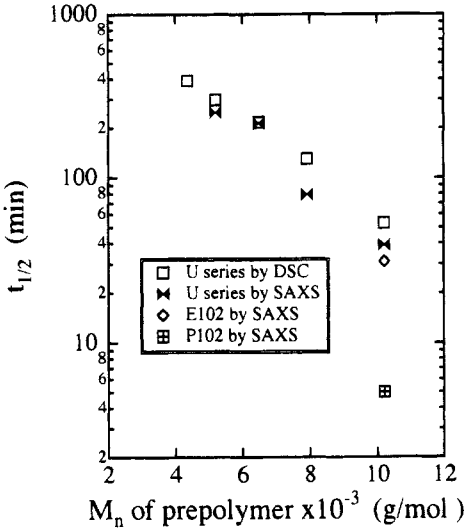

Figure 8. M_n dependence of crystallization half-time, $t_{1/2}$ for PTHF networks (U series) and the corresponding polymers, E102 (chain-extended linear polymer) and P102 (prepolymer).

for the prepolymer (P102) is about 1 order of magnitude smaller than that for U102. Thus it is obvious that the presence of cross-links greatly suppresses the rate of crystallization by a factor of 10 in this particular case. The effect of chain extension, i.e., E102, is also significant, indicating that not only the topology of the polymer chain but also the length are important factors which affect the crystallization rate.

2. Morphology of PTHF Networks. Figure 9 shows a series of optical micrographs of the U065 PTHF network taken under cross-nicol polarization. At t = 20 min (a), a few numbers of spherulites are formed. As time goes on, the spherulites grow in size to certain values and then start to impinge. Note that clear Maltese crosses are observed in (b) and the number of spherulites is rather constant with t. Thus an instantaneous crystallization takes place in this system.

Figure 10 shows the crystallization time, t, dependence of the spherulite diameter for U065. Among many spherulites observed under a polarized microscope, five spherulites were arbitrarily chosen and their diameters were observed as a function of time. In this way, the linear growth rate of the spherulite (indicated with the dashed line) was evaluated to be 641 nm/min. As shown in the figure, the spherulite diameter increased linearly with t. From Figures 9 and 10, it can be concluded that an instantaneous crystallization occurs in this experimental condition. In this region, network chains seem to be relatively mobile. At a later stage, a slowing down of the crystallization rate is expected to occur due to straining of the remaining part of the network. However, such behavior is not found in this time range.

Discussion

On the basis of the results shown above, we now discuss the origin of the slow crystallization observed in the PTHF networks and the inter-cross-link molecular weight, M_n (or x_n), dependence of the crystallization kinetics.

1. Thermodynamics of Isothermal Crystallization. First of all, we evaluate the equilibrium melting temperature, $T_m°$, since the observed melting temperature, T_m, is dependent on the crystallization temperature, T_C. Since $T_m°$ is related to the lamellar thickness, d, it should be evaluated on the basis of SAXS re-

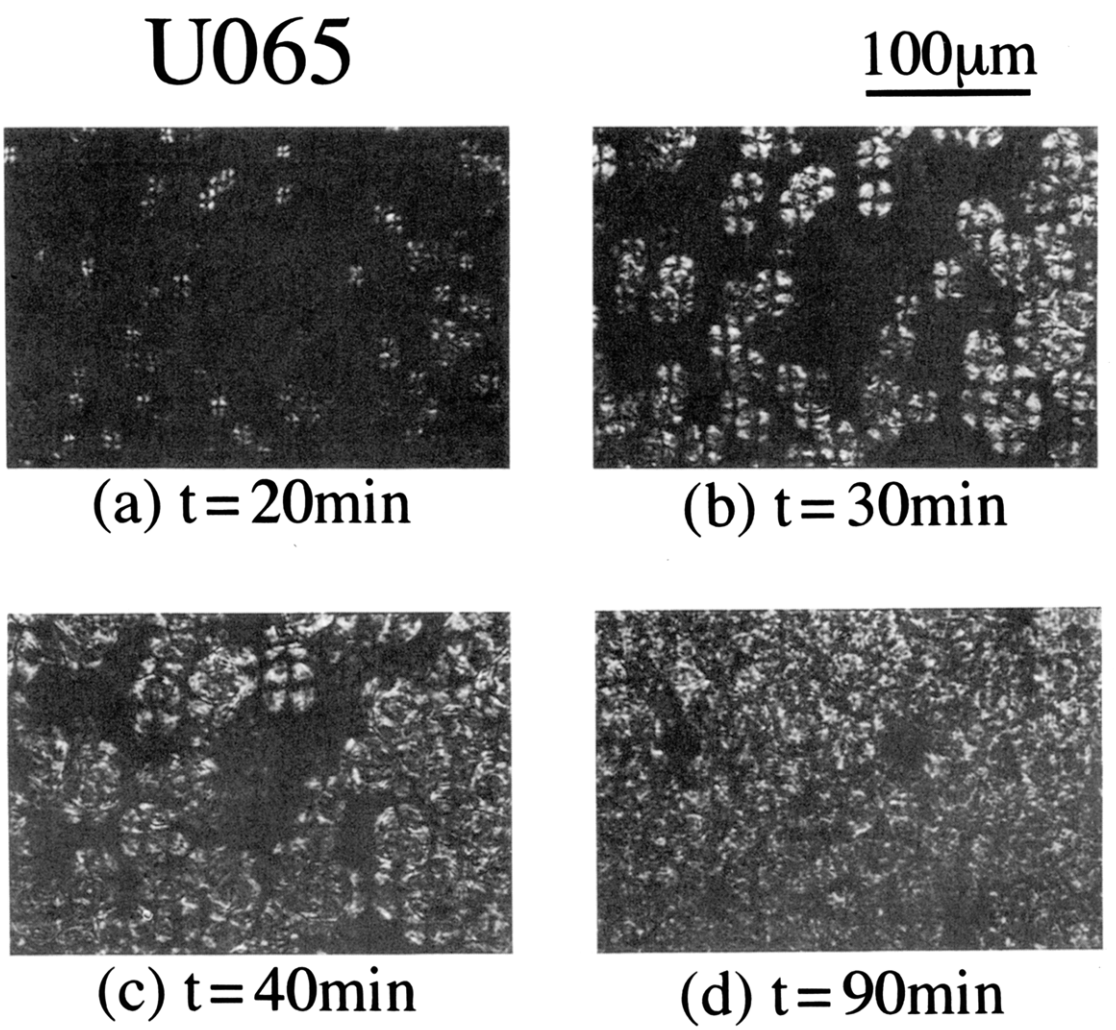

Figure 9. Series of cross-polarized optical micrographs of U065 network films crystallized for t = (a) 20, (b) 30, (c) 40, and 90 min at 15 °C. Polarization directions are vertical and horizontal.

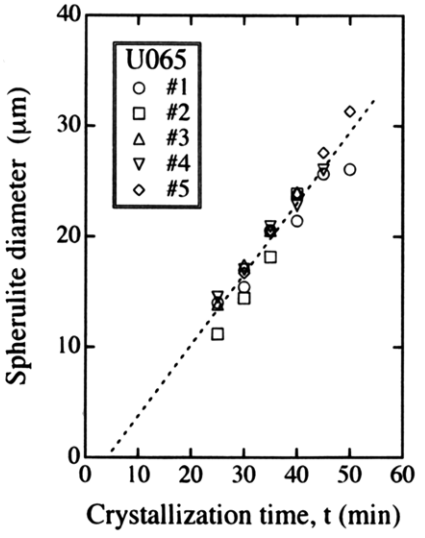

Figure 10. Variation of spherulite diameter for U065 as a function of crystallization time, t.

sults,[17,18] i.e., from the T_m vs $1/d$ plot. However, measurements of crystal thickness at various T_C could not be carried out because of limitations of the SAXS beam time and difficulty in avoiding an annealing effect. Note that samples have to be kept at a temperature much lower than T_m (~30 °C) after crystallization at T_C and a SAXS experiment has to be conducted at the temperature. Thus a Hoffman–Weeks[19] plot analysis was employed to estimate $T_m°$. The problems related to the Hoffman–Weeks plot analysis, such as kinetic effect and lamellar thickening effect on T_m, are extensively discussed by Phillips and co-workers[17] and by Manderkern.[18] Figure 11 shows the Hoffman–Weeks plots of (a) PTHF prepolymers and (b) networks. The thick dashed line indicates $T_m = T_C$. Although the number of data points is limited, the experimental data points can be extrapolated to higher temperatures and $T_m°$ was estimated at the marginal point with the $T_m = T_C$ line. According to these plots, it is clear that $T_m°$ decreases with decreasing M_n (or x_n). It should be noted here the estimated value of $T_m°$ is definitely an overestimation since both prepolymers and networks are in the molten state at 60 °C. Therefore, for accurate determination of $T_m°$, it is necessary to conduct a SAXS experiment for crystallization at different T_C's, which will be a future work. Knowing this fact, we continue discussions about the thermodynamics of the crystallization of the PTHF network.

In the case of linear polymers, the equilibrium melting temperature, $T_m°$, is a function of the degree of polymerization, x_n, due to the presence of chain ends, and the following relation is given:[20]

$$\frac{1}{T_m°(x_n)} - \frac{1}{T_m°(\infty)} = \frac{R}{\Delta H_u}\frac{2}{x_n} \tag{4}$$

where R is the gas constant and $T_m(\infty)$ is the melting

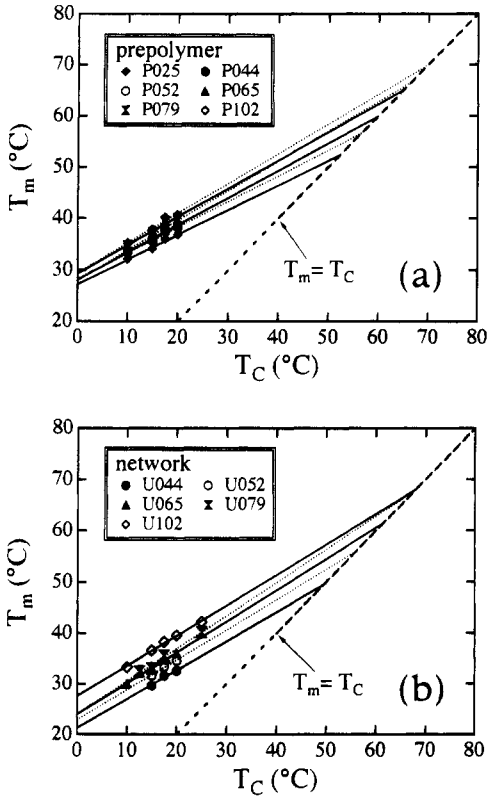

Figure 11. Hoffman–Weeks plots of (a) PTHF prepolymers and (b) networks. The dashed line indicates the line for $T_m = T_C$.

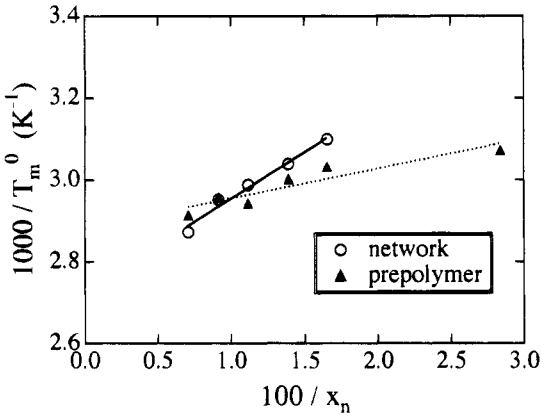

Figure 12. Variation of inverse melting temperature, $1/T_m°$, as a function of $1/x_n$.

temperature for polymers having infinite molecular weight. ΔH_u is the enthalpy of fusion per monomeric unit of the polymer. It is assumed here that both chain ends do not participate in crystallization and are excluded from the crystalline phase. In the case of polymer networks, eq 4 can be rewritten to

$$\frac{1}{T_m°(x_n)} - \frac{1}{T_m°(\infty)} = \frac{R}{\Delta H_u}\frac{2C}{x_n} \qquad (5)$$

where C is the additional constraint factor due to the steric hindrance related to cross-links.

Figure 12 shows the reciprocal melting temperature, $1/T_m°(x_n)$ vs $1/x_n$ for PTHF prepolymers (dashed line) and networks (solid line). As expected from eqs 4 and 5, a linear relaticnship is found both for the prepolymers and networks. Thus a systematic melting point depression with x_n occurs due to the presence of chain ends (prepolymer) or cross-links (network), and the effect of

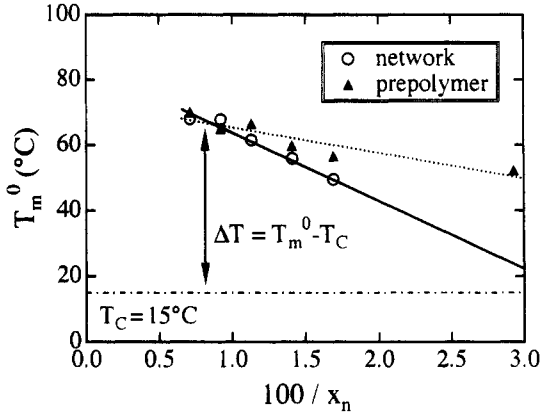

Figure 13. Variation of equilibrium melting temperature, $T_m°$, as a function of $1/x_n$. The crystallization temperature, T_C, is also shown with a dash–dot line.

a cross-link is much stronger than that of the others. The value of ΔH_u was estimated to be 2.3 kJ/mol for prepolymers, which is smaller than the literature value,[21] 12.6 kJ/mol, by a factor of about 5.5. This disagreement is definitely from an overestimation of $T_m°$. Note that two lines should merge at $1/x_n = 0$. The result does not agree to this prediction, which is again due to the overestimation. Anyway, by taking the ratio of the slopes, we estimated the additional constraint factor, C, to be 3.1. This indicates that three THF segments next to a cross-link are excluded per cross-link from a crystallite on crystallization.

Figure 13 shows the variation of $T_m°$ as a function of $1/x_n$ for PTHF prepolymers (dashed line) and networks (solid line). The crystallization temperature, T_C, was also indicated with a dash-dotted line for comparison. As shown here, $T_m°$ for the networks is a strong decreasing function of $1/x_n$. Therefore an isothermal crystallization at T_C = 15 °C means that PTHF networks having different x_n's were crystallized at a condition of different supercooling, ΔT. Since the x_n dependence of $T_m°$ is very strong, the crystallization kinetics of PTHF networks was a strong function of x_n. For example, this is why U025 crystallizes at 0 °C but not at 15 °C. On the other hand, such a strong dependence of ΔT on x_n was not found in the prepolymers, as shown by the dashed line. This systematic variation of $T_m°$ implies that the degrees of supercooling on isothermal crystallization are different in the samples having different M_n.

2. Crystallization Kinetics. Crystallization kinetics is often analyzed phenomenologically by the Avrami equation,[20,22]

$$\ln\left[-\ln\left(\frac{X_\infty - X_t}{X_\infty}\right)\right] = \ln k + n \ln t \qquad (6)$$

where X_t and X_∞ are the degree of crystallization at time t and that at equilibrium. The parameters k and n are the crystallization rate constant and the Avrami exponent, respectively. Figure 14 shows the so-called Avrami plots, $\ln\{-\ln[(X_\infty - X_t)/X_\infty]\}$ vs $\ln t$, for $X = A$. The exponent n is in the range from 2.2 to 2.4, although the n value for U102 is exceptionally larger than the others. It is interesting to compare the Avrami exponents of E102 (chain-extended linear polymer) and P102 (prepolymer). For E102, the exponent is close to the networks (U series), while P102 has a larger n value. This tendency is the same as that of the crystallization half-time, $t_{1/2}$. Phillips et al. reported similar results

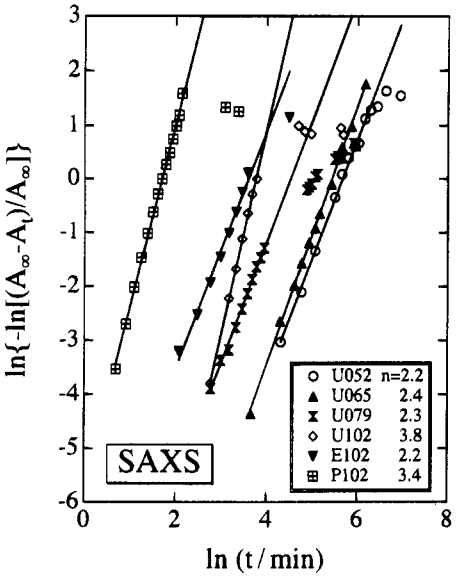

Figure 14. Avrami plots for the PTHF network based on the results of SAXS integrated intensity.

for linear ($n \approx 3$) and cross-linked polyethylenes ($n \approx 2$ to $n \approx 2.5$).[2]

3. Crystallization Mechanism of End-Linked Polymer Networks. In the previous paper, we discussed crystallization kinetics of U052 crystallized at 20 °C, where the sol fraction was not extracted, and concluded that the crystallization of the PTHF network was characterized by homogeneous nucleation, diffusion control, and three-dimensional growth based on the Avrami exponent being around 2.[4] However, the observation of a linear growth of spherulites shown in Figure 9 supports the fact that the crystal growth mechanism is not diffusion controlled by an interface-limited process.[20,22] Figure 8 also indicates that nucleation of spherulites seems to be instantaneous with time and randomly located in space.

Invariance of L with x_n, observed by SAXS, and the presence of spherulites indicates that the crystallites in the network are formed by folded chains rather than extended chains or fringed micelles.

The obtained Avrami exponent, which is ~2, may be explained as follows: If the spherulite is densely packed with stacks of crystalline lamellae, one expects the space dimension, $D = 3$, and $n = D = 3$ for instantaneous nucleation. This is explained by deducing that spherulites in the early stage are very coarse. In other words, if skeleton spherulites are formed due to the topological constraint in the network, it is not necessary to represent the crystallization kinetics by $n = 3$. Actually, the degree of completion of crystallization of U052 was about 30–40% of P052 when crystallized at 20 °C.[4] Since the observed regime of crystallization is in the early stage before the start of impingement of the spherulites, it is reasonable for n to be smaller than 3. The validity of this speculation will be checked by studying the crystallization kinetics at various crystallization temperatures coupled with modern theories of polymer crystallization.[23–25]

Concluding Remarks

Studies on crystallization kinetics of PTHF networks having well-defined inter-cross-link molecular weights, M_n, disclosed the following facts: (1) End-linked PTHF networks are crystallizable, having the long period of ~200 Å. The long period was roughly invariant against M_n in the molecular weight range studied here. (2) A spherulite superstructure was observed in spite of the presence of cross-links. The spherulite growth rate was linear with time. (3) The crystallization rate is a strong function of M_n, and the rate decreases with decreasing M_n. (4) The Avrami exponent, n, for PTHF networks is significantly lower than a predicted value for instantaneous crystallization, which is explained as formation of coarse crystals due to cross-links. (5) The decrease in the crystallization rate with decreasing inter-cross-link molecular weight, M_n, is accounted for by a decrease of the supercooling.

Acknowledgment. The authors are indebted to Prof. Richard S. Stein, University of Massachusetts at Amherst, and Prof. T. Okui, Tokyo Institute of Technology, for fruitful discussions. The authors appreciate the helpful suggestions made by the reviewers. This work was performed with the approval of the Photon Factory Program (93G245).

References and Notes

(1) Phillips, P. J.; Kao, Y. H. *Polymer* **1986**, *27*, 1679.
(2) Phillips, P. J.; Lambert, W. S. *Macromolecules* **1990**, *23*, 2075.
(3) Lambert, W. S.; Phillips, P. J.; Lin, J. S. *Polymer* **1994**, *35*, 1809.
(4) Shibayama, M.; Takahashi, H.; Yamaguchi, H.; Sakurai, S.; Nomura, S. *Polymer* **1994**, *35*, 2944.
(5) Cruz, C. S.; Stribeck, N.; Zachmann, J. G. *Macromolecules* **1991**, *24*, 5980.
(6) Wang, J.; Alvarez, M.; Zhang, W.; Wu, Z.; Li, Y.; Chu, B. *Macromolecules* **1992**, *25*, 6943.
(7) Bourgaur, C.; Paternostre, L.; Dosiere, M. *J. Phys. IV, Colloq. C8*, **1993**, *3*, 29.
(8) Tashiro, K.; Satkowski, M. M.; Stein, R. S.; Li, Y.; Chu, B.; Hsu, S. L. *Macromolecules* **1992**, *25*, 1809.
(9) Nojima, S.; Kato, K.; Ono, M.; Ashida, T. *Macromolecules* **1992**, *25*, 1922.
(10) Nojima, S.; Kato, K.; Yamamoto, S.; Ashida, T. *Macromolecules* **1992**, *25*, 2237.
(11) Jong, L.; Stein, R. S. *Macromolecules* **1991**, *24*, 2323.
(12) Ueki, Y.; Hiragi, Y.; Kataoka, M.; Inoko, Y.; Amemiya, Y.; Izumi, Y.; Tagawa, H.; Muroga, Y. *Biophys. Chem.* **1985**, *23*, 115.
(13) Dreyfuss, P. *Polytetrahydrofuran*; Gordon and Breach Science: New York, 1982.
(14) Hashimoto, M.; Shibayama, M.; Takahashi, H.; Nomura, S. Manuscript in preparation for publication.
(15) Shibayama, M.; Nomura, S.; Hashimoto, T.; Thomas, E. L. *J. Appl. Phys.* **1989**, *66*, 4188.
(16) Strobl, G. R.; Schneider, M. *J. Polym. Sci., Polym. Phys. Ed.* **1980**, *18* 1343.
(17) Mezghani, K.; Campbell, A.; Phillips, P. J. *Macromolecules* **1994**, *27*, 997.
(18) Mandelkern, L. *Comprehensive Polymer Science*; Pergamon Press: Oxford, U.K.; **1989**; Vol. 2.
(19) Hoffman, J. D.; Weeks, J. J. *J. Chem. Phys.* **1965**, *42*, 4301.
(20) Mandelkern, L. *Crystallization of Polymers*; McGraw Hill: New York, 1964.
(21) Brandrup, J., Immergut, E. H., Eds. *Polymer Handbook*, 3rd ed.; Wiley: New York, 1989.
(22) Schultz, J. *Polymer Materials Science*; Prentice-Hall: Englewood Cliffs, NJ, 1974.
(23) Clark, E. J.; Hoffman, J. D. *Macromolecules* **1984**, *17*, 878.
(24) Hikosaka, M. *Polymer* **1987**, *28*, 1257.
(25) Hikosaka, M. *Polymer* **1990**, *31*, 458.

MA946328S